

Electron binding energies of hydrated H_3O^+ and OH^- : Photoelectron spectroscopy of aqueous acid and base solutions combined with electronic structure calculations

Bernd Winter,^{1*} Manfred Faubel,² Ingolf V. Hertel,¹ Christian Pettenkofer,³ Stephen E. Bradforth,^{4*} Barbara Jagoda-Cwiklik,⁵ Lukasz Cwiklik,⁵ Pavel Jungwirth^{5*}

¹Max-Born-Institut für Nichtlineare Optik und Kurzzeitspektroskopie, Max-Born-Str. 2A, D-12489 Berlin, Germany, ²Max-Planck-Institut für Dynamik und Selbstorganisation, Bunsenstr. 10, D-37073 Göttingen, Germany, ³Hahn-Meitner-Institut, Glienickerstr. 100, D-14109 Berlin, Germany, ⁴Department of Chemistry, University of Southern California, Los Angeles, California 90089, ⁵Institute of Organic Chemistry and Biochemistry, Academy of Sciences of the Czech Republic, and Center for Biomolecules and Complex Molecular Systems, Flemingovo nám. 2, 16610 Prague 6, Czech Republic.

Received ...; E-mail: bwinter@mbi-berlin.de (B.W.); bradforth@usc.edu (S.E.B.); pavel.jungwirth@uochb.cas.cz (P.J.)

The ability of water molecules to spontaneously dissociate into hydronium and hydroxide ions is arguably the most important chemical property of liquid water, which is behind all pH-related phenomena. Despite an immense interest in the ionic product of water, and spectacular progress in experimental and computational description of its structure and dynamics, many open questions remain.¹ Recently, a lot of effort has been devoted to elucidating the proton transfer mechanism in hydrated H_3O^+ and OH^- .^{2,3} The goal of the present work is complementary to these studies. By means of EUV photoelectron spectroscopy of aqueous acid and base solutions, supported by *ab initio* and molecular dynamics calculations, we characterize the electron binding energies for the hydronium and hydroxide ions. This is the first time experimental data on the aqueous phase electronic structure of these ubiquitous ions are reported and interpreted.

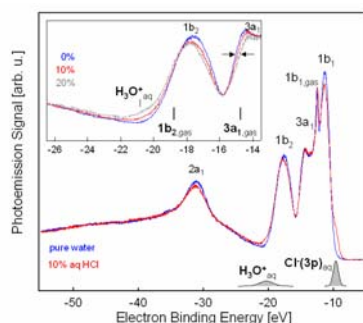


Figure 1: PE spectra of 10 wt% (3m) aq HCl and of pure liquid water, measured at 100 eV photon energy (intensities are normalized to photon flux). Water orbital features and the major H_3O^+ and Cl^- contributions are indicated. Inset: enlargement of the H_3O^+ region; data for 20% (6.8m) aq HCl are also included. Lines locate the gas-phase water positions.

The photoemission (PE) experiments were performed at BESSY, using a 10 μm liquid jet, the experimental setup being described in detail elsewhere.⁴ All spectra presented here were obtained for 100 eV photon energy, corresponding to 5-10 \AA electron inelastic mean free path,⁵ hence both bulk and surface emissions contribute to the spectra. Fig. 1 shows the PE spectrum of pure liquid water, and that of 3m aqueous HCl solution. Water signal decrease in the acid spectrum is due to reduced water concentration. Hydrated $\text{Cl}^-(3p)$ gives rise to the lowest energy feature at 9.6 eV. A clearly discernible emission from the hydrated proton is the small peak at 20 eV. In addition, the absence of water signal decrease for the $3a_1$ orbital, near 14 eV, suggests additional, unresolved H_3O^+ emission at this energy. This effect increases proportionally to the H_3O^+ concentration (inset to Fig. 1). Note also the apparent peak narrowing near the high-energy side of the $3a_1$ feature, indicated by arrows, which results from the reduced vapor pressure at higher concentration.

For the $1b_2$ contribution this effect is masked by strong 20 eV H_3O^+ emission, increasing for higher concentration.

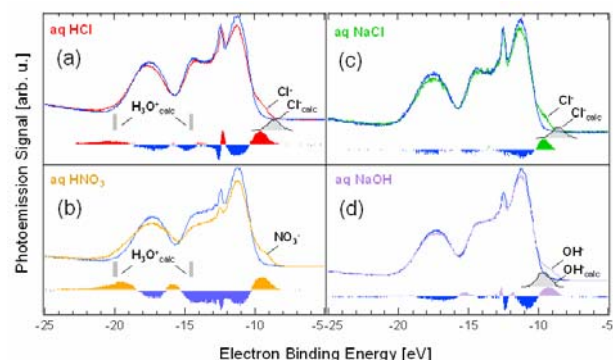


Figure 2: Photoemission spectra of aqueous solutions of (a) 3m HCl, (b) 4m HNO_3 , (c) 3m NaCl, and (d) 2m NaOH. For comparison the pure water PE spectra and the differential spectra are also shown. Solute emission contributions can be identified as the positive contributions in the difference spectra. Gray shaded features indicate the calculated ionization energies of (a,b) H_3O^+ , and PE bands for (a,c) Cl^- ,⁴ and (d) OH^- . The calculated widths for the anionic bands are drawn to scale.

Fig. 2 compares the 3m aq HCl PE spectrum with those of aq HNO_3 , aq NaCl, and aq NaOH, all at similar concentrations. In each case the specific anion emission gives rise to the lowest energy shoulder. As expected, the nitric acid spectrum also exhibits a pronounced peak at 20 eV; the broadening and shift of this feature, and also the extra intensity at 16 eV presumably result from contributions from the more complex NO_3^- spectrum. Our assignment of the 20 eV peak to H_3O^+ is further supported by the absence of this feature in NaCl and NaOH solutions. Both of these spectra are nearly identical with the corresponding water spectrum, except for the water intensity decrease and the emerging Cl^- or OH^- features. The OH^- peak appears at 9.2 eV, with 1.15 eV fwhm. The chloride peak position observed in HCl is identical to that in alkali chloride solutions (at 9.6 eV).⁵

In our previous study of aqueous salt solutions we have explored various computational approaches to evaluating electron binding energies of solvated ions.⁶ We have shown that for anions a viable computational strategy consists of running first a classical molecular dynamics (MD) simulation of a single anion in a periodic box of water molecules. The vertical ionization potential (IP) is then evaluated *ab initio* as a difference between the anionic and neutral energies sampling the series of water

configuration from the MD trajectory, with water molecules represented by fractional charges. For positively charged ions this approach, however, overestimates the IPs due to the neglect of solvent electronic polarization, which is particularly important for stabilizing the nascent dication. As a matter of fact, much better results were obtained for alkali cations using a polarizable continuum model (PCM) for the solvent, despite the implicit relaxation of the solvent nuclear polarization.⁶

Based on this experience⁶ we have run a 1 ns MD trajectory (1 fs time step, 300 K) for a single rigid OH⁻ ion in a periodic box containing 555 SPC/E water molecules.^{7,8} Long range electrostatic interactions beyond the 12 Å cutoff were accounted for via the particle-mesh Ewald procedure.⁹ 1000 snapshots, separated by 1 ps, provided input for consequent MP2/aug-cc-pVTZ calculations of the OH⁻ vertical IP, with water molecules closer than 12 Å from the anion included as partial charges (-0.82 on O and 0.41 on H atoms). MD and *ab initio* calculations were performed using Amber 6 and Gaussian 03, respectively.^{10,11}

The resulting distribution of IPs (from detachment from either of the two $2p\pi$ orbitals of OH⁻), peaking at 9.7 eV is depicted in gray in Fig. 2(d). The local asymmetry of the solvent splits the degeneracy of the $2p\pi$ by 0.2 eV, but the inhomogeneity in solvent sites provides most of the peak broadening (0.9 eV). The next IP is at 13.5 eV, and corresponds to removal of the $2p\sigma$ electron. Unfortunately, this peak is hidden in the experiment under the strong water structure. For ten representative geometries we also included the first solvation shell around OH⁻ (four water molecules on average) quantum mechanically. This results in a 0.1-0.2 e charge transfer from OH⁻ to neighboring waters, but has a minor effect on the IP (average blue shift of less than 0.2 eV).

As for the alkali cations,⁶ we have evaluated the electron binding of the aqueous cation by embedding H₃O⁺ (implicitly assuming the prevalence of Eigen-like structures for the hydrated proton¹²) using a PCM for the solvent. Strictly speaking, the PCM approach gives adiabatic IPs. However, as we have deduced for alkali cations, the difference between adiabatic and vertical IPs is small in this case due to a similar arrangement of water molecules around the cation and the corresponding dication. We have evaluated the lowest IP of H₃O⁺ at the MP2/aug-cc-pVTZ level (employing the gas phase geometry, optimized at the same level of theory), while the higher ionization potentials were estimated using TD-B3LYP calculations for the dication using the same basis set. The lowest IP lies at 14.5 eV (Fig. 2), and reflects ionization from the highest ($3a_1$) p-orbital of H₃O⁺. The next IP at 19.8 eV corresponds to ionization from the degenerate set of the remaining two valence ($1e$) p-orbitals, while the following IP of 32.3 eV correlates with the removal of a valence ($2a_1$) s-electron. For comparison, we also tested the Zundel H₅O₂⁺ structure of the hydrated proton; a strong shift (by more than 2 eV) to lower IP is observed compared to the Eigen core.

The present calculations are complementary to the Car-Parrinello MD simulations of hydrated hydronium and hydroxide ions.¹³ Those simulations account for the electronic structure of the whole system, thus opening a window for the description of important phenomena of proton delocalization and hopping in water. However, within that approach it is very difficult to calculate IPs as energy differences between electronic states before and after electron removal, particularly for cases where the final state is an excited state of the whole system. The IPs must then be estimated from the local density of states, based on the one electron Kohn-Sham orbitals. However, the application of the Koopman's theorem in density functional theory is not well justified and leads to sizable errors. For example, the computed

positions of the H₃O⁺, OH⁻, and water peaks^{13,14} are all shifted by 3-5 eV to lower IPs compared to the present experiments. Within our approach, where electronic structure calculations of the relevant states of the solute account for the solvent approximately either as fractional charges (aq OH⁻) or within a polarizable continuum model (aq H₃O⁺), we avoid issues of charge transfer relaxation in the final states and can, therefore, focus on the vertical IP without resort to Koopman's theorem. As a result, we are obtaining IPs closer to experiment, although it is clear that we still neglect important aspects of the solute-solvent interactions and have to invoke different approaches for the anion and cation.

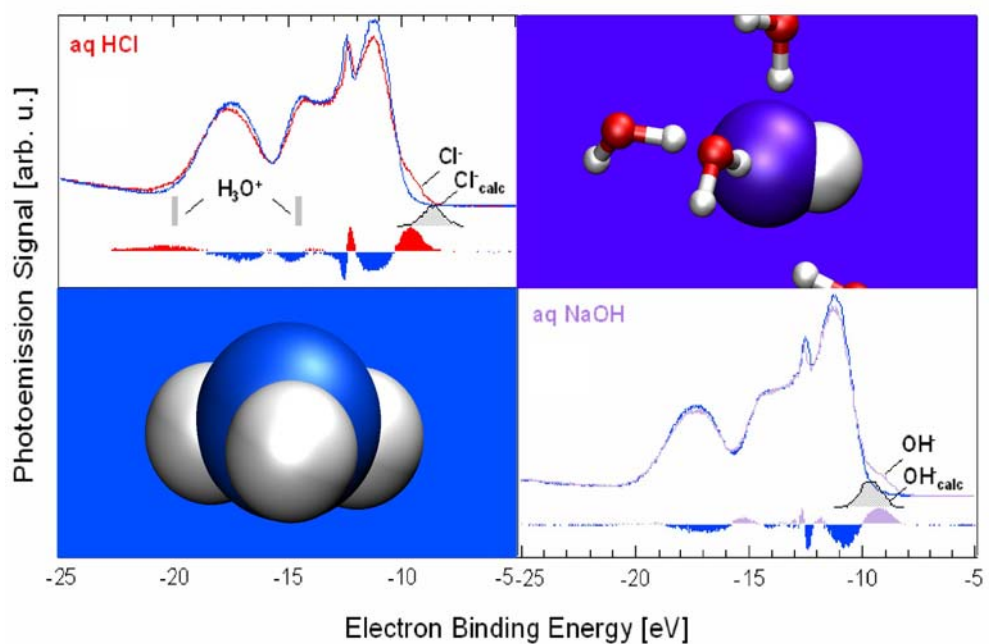
Several of the solute lines are obscured by water features in the experiment. However, spectral signatures of the lowest IP of OH⁻ at 9.2 eV and of the second lowest IP of H₃O⁺ at 20 eV are clearly resolved and are both in a very good agreement with the present calculations. The present peak position and width for OH⁻ is also consistent with a previously determined threshold energy of 8.45 eV.¹⁵ The observed IP of hydronium is in better agreement with calculations which assume an Eigen rather than a Zundel core. Note that our calculations are pertinent to the bulk, while the experiment samples both bulk and surface regions. Our recent simulations indicate that in base solutions OH⁻ is weakly repelled from the surface, while in acid solutions H₃O⁺ shows a weak propensity for the surface.¹⁶ Given the experimental probing depth, we suggest that the signal therefore originates predominantly from completely or almost completely solvated ions. Moreover, earlier work suggests that ionic IPs in the interfacial layer may be similar to those in the aqueous bulk.¹⁷

The results presented here fill a gap in our knowledge on the electronic properties of hydrated H₃O⁺ and OH⁻. The existing thermodynamic, spectroscopic, and computational data on the ionic product of water are complemented by first reliable values for the ionization potentials. We also believe that these results will provide a useful calibration point for developing quantitative *ab initio* molecular dynamics models for ions in water.

Acknowledgement: We thank Ramona Weber and Wolfgang Freyer for experimental assistance. Support from the EU (contract RII-CT-2003-506350, Laserlab Europe), from the Czech Ministry of Education (grants LC512 and ME644) and NSF (CHE 0431512 and 0209719) to PJ, and from the NSF (CHE-0311814) and the Packard Foundation to SEB is gratefully acknowledged.

References:

- Geissler, P. L.; Delago, C.; Chandler, D.; Hutter, J.; Parrinello, M. *Science* **2001**, *291*, 2121.
- Agmon, N. *J. Phys. Chem. A* **2005**, *109*, 13 and references therein.
- Chen, B.; Ivanov, I.; Park, J.-M.; Parrinello, M.; Klein, M. L. *J. Phys. Chem. B* **2002**, *106*, 12006 and references therein.
- Winter, B.; Weber, R.; Widdra, W.; Dittmar, M.; Faubel, M.; Hertel, I. V. *J. Phys. Chem. A* **2004**, *108*, 2625.
- Faubel, M. Photoelectron Spectroscopy at Liquid Surfaces. In *Photoionization and Photodetachment*, part I; Ng, C.-Y., Ed.; World Scientific: Singapore, 2000; p. 634.
- Winter, B.; Weber, R.; Hertel, I. V.; Faubel, M.; Jungwirth, P.; Brown, E. C.; Bradforth, S. E. *J. Am. Chem. Soc.* **2005**, *127*, 7203.
- Berendsen, H. J. C.; Grigera, J. R.; Straatsma, T. P. *J. Phys. Chem.* **1987**, *91*, 6269.
- Brodskaya, E.; Lyubartsev, A. P.; Laaksonen, A. *J. Phys. Chem. B* **2002**, *106*, 6479.
- Essmann, U.; Perera, L.; Berkowitz, M. L.; Darden, T.; Lee, H.; Pedersen, L. G. *J. Chem. Phys.* **1995**, *103*, 8577.
- Case, D. A. et al., *AMBER 6*, University of California, San Francisco 1999.
- Frisch, M. J. et al., *Gaussian 03 (Revision C.02)*, Gaussian Inc.: Wallingford, CT 2004.
- Schmitt, U. W.; Voth, G. A. *J. Chem. Phys.* **1999**, *111*, 9361.
- Tuckerman, M.; Laasonen, K.; Sprik, M.; Parrinello, M. *J. Chem. Phys.* **1995**, *103*, 150.
- Hunt, P.; Sprik, M.; Vuilleumier, R. *Chem. Phys. Lett.* **2003**, *376*, 68.
- vonBurg, K.; Delahay, P. *Chem. Phys. Lett.* **1981**, *78*, 287.
- Mucha, M.; Frigato, T.; Levering, L.; Allen, H. C.; Tobias, D. J.; Dang, L. X.; Jungwirth, P. *J. Phys. Chem. B* **2005**, *109*, 7617.
- Bradforth, S. E.; Jungwirth, P. *J. Phys. Chem. A* **2002**, *106*, 1286.



ABSTRACT FOR WEB PUBLICATION (Word Style "BD_Abstract"). Authors are required to submit a concise, self-contained, one-paragraph abstract for Web publication.

The electronic structure of hydrated H_3O^+ and OH^- is probed in a water jet by photoelectron spectroscopy employing 100 eV photons. The first ionization potential for OH^- at 9.2 eV and the second ionization potential for H_3O^+ at 20 eV are resolved corresponding to the removal of an electron from the $2p\pi$ highest occupied molecular orbital and from the $1e$ orbital, respectively. These assignments are supported by present computational results based on a combination of molecular dynamics and *ab initio* calculations.